EAST EUROPEAN JOURNAL OF PHYSICS. **2.** 335-341 (2025)
DOI:10.26565/2312-4334-2025-2-42 ISSN 2312-4334

Zn_2SnO_4 THIN FILMS FOR PHOTOVOLTAICS: STRUCTURAL OPTIMIZATION AND CHARGE TRANSPORT ANALYSIS

Fakhriddin T. Yusupov*, Tokhirbek I. Rakhmonov, Dadakhon Sh. Khidirov, Shakhnoza Sh. Akhmadjanova, Javokhirbek A. Akhmadaliyev
Fergana State Technical University, Fergana, Uzbekistan
**Corresponding Author e-mail: yusupov.fizika@gmail.com*
Received February 5, 2025; revised April 2, 2025; accepted April 12, 2025

In this study, (Zn,Sn)O thin films were synthesized and characterized for potential application as buffer layers in photovoltaic devices. The films were deposited using thermal evaporation in a high-vacuum chamber, followed by a controlled oxidation process in a pure oxygen atmosphere to achieve a ZnO-based oxide layer. Post-deposition annealing was conducted at various temperatures (400°C-550°C) to enhance crystallinity and phase composition. X-ray diffraction (XRD) analysis confirmed the formation of a highly crystalline Zn_2SnO_4 phase, with the optimal structure obtained at 550°C. Optical characterization revealed a temperature-dependent bandgap narrowing effect, significantly influencing transmittance and reflectance spectra. Electrical properties were assessed via Hall effect and current-voltage (I-V) measurements, indicating an increase in carrier mobility and conductivity at higher annealing temperatures. The charge transport mechanism in Ni-(Zn,Sn)O-pSi-Ni heterostructures was analyzed using the space-charge-limited current (SCLC) model, revealing that carrier injection is the dominant transport process. The results demonstrate that (Zn,Sn)O thin films exhibit superior optoelectronic properties, making them promising candidates for photovoltaic and optoelectronic applications.
Keywords: *(Zn,Sn)O thin films; Photovoltaic applications; Thermal evaporation; X-ray diffraction; Optical properties; Electrical transport; Hall effect; Charge carrier mobility; Heterostructures*
PACS: 78.20.-e, 73.61.Ga, 85.60.-q, 68.55.-a

INTRODUCTION

The continuous advancement in photovoltaic (PV) technology demands the development of highly efficient and stable materials for next-generation solar cells. Among various oxide semiconductors, Zn_2SnO_4 (zinc stannate) thin films have emerged as promising candidates due to their wide bandgap, excellent optical transmittance, and superior charge transport properties [1]. These characteristics make Zn_2SnO_4 an attractive alternative to conventional buffer layers in PV devices, potentially improving light absorption and charge carrier dynamics at the heterojunction interface. The performance of Zn_2SnO_4 thin films is heavily influenced by deposition techniques, annealing processes, and compositional tuning [2]. Thermal evaporation followed by controlled oxidation in an oxygen-rich environment enables precise structural and electronic tailoring, enhancing their suitability for optoelectronic applications. Notably, post-deposition annealing plays a crucial role in modifying crystallinity, phase composition, and defect states - factors that significantly impact electrical conductivity and band alignment. Despite its potential, optimizing the electronic and optical behavior of Zn_2SnO_4 remains a challenge, primarily due to the complex interplay between defect formation, charge carrier mobility, and bandgap engineering [3]. This study systematically investigates the structural, optical, and electrical properties of (Zn,Sn)O thin films, deposited via high-vacuum thermal evaporation and subjected to post-deposition annealing at various temperatures (400°C–550°C). By employing X-ray diffraction (XRD), UV-Vis spectrophotometry, Hall effect measurements, and current-voltage (I-V) analysis, we explore the impact of annealing on phase purity, carrier transport, and optoelectronic performance. Additionally, the charge transport mechanisms in Ni-(Zn,Sn)O-pSi-Ni heterostructures are analyzed using the space-charge-limited current (SCLC) model, providing deeper insights into carrier injection and conduction behavior.

The findings presented in this work contribute to the ongoing efforts in semiconductor material optimization for photovoltaic applications. By understanding the role of annealing and charge transport dynamics, we aim to establish Zn_2SnO_4 as a viable buffer layer material, paving the way for enhanced light conversion efficiency and long-term stability in solar cell architectures [2].

EXPERIMENTAL METHODOLOGY

The deposition of (Zn, Sn)O thin films was carried out in a high-vacuum chamber, where a controlled atmosphere was maintained by evacuating air and subsequently introducing a precise mixture of argon and oxygen gases. In our previous studies [4-6], we have employed this method to investigate the electro-physical and optical properties of both pure zinc oxide and doped zinc oxide thin films. In this regard, various techniques, including physical methods such as RF sputtering [7,8] and chemical approaches like spray pyrolysis [9,10], have been reported for the fabrication of ZTO thin films. This study focuses on the thermal oxidation process, in which Zn-Sn thin films, deposited via thermal

Cite as: F.T. Yusupov, T.I. Rakhmonov, D.Sh. Khidirov, Sh.Sh. Akhmadjanova, J.A. Akhmadaliyev, East Eur. J. Phys. 2, 335 (2025), https://doi.org/10.26565/2312-4334-2025-2-42

evaporation, undergo oxidation in a pure oxygen atmosphere, forming a ZnO-based oxide layer. The method was applied to different substrates, including silicon, sapphire, and glass to evaluate the feasibility of fabricating heterostructures for optoelectronic and photovoltaic applications.

The deposition parameters were optimized to ensure the formation of nanocrystalline ZnO thin films with a preferential c-axis orientation, an essential factor in enhancing their optoelectronic and electrical properties. The substrate temperature was maintained at 200°C and the working pressure of the $Ar+O_2$ gas mixture was regulated at 2.3×10^{-2} Pa. The thickness of the ZnO films, ranging from 1.5–2 μm, was precisely controlled using a quartz crystal thickness monitor (IC5) [5].

Following deposition, the films underwent post-deposition thermal annealing in air at different temperatures (400°C, 450°C, 500°C, and 550°C) for 2 hours to promote oxidation and improve crystallinity. The annealing process facilitated the transformation of the Sn/Zn bilayer into a well-defined Zn_2SnO_4 phase while optimizing its structural, electrical, and optical properties. The structural characterization of the annealed films was conducted using X-ray diffraction (XRD) with Cu Kα radiation (λ = 1.5406 Å) to analyze the phase composition, crystallinity, and preferential orientation. The average crystallite size was determined using the Debye-Scherrer equation. The optical properties were investigated through UV-Vis spectrophotometry over a wavelength range of 200–1500 nm, measuring optical transmittance and reflectance to determine the bandgap energy [11].

Electrical properties were characterized using Hall effect measurements and current-voltage (I-V) characterization. The carrier concentration, resistivity, and Hall mobility were determined using a four-probe setup. The I-V characteristics of Ni-(Zn, Sn)O-pSi-Ni heterostructures were recorded at temperatures ranging from 350°C to 550°C to evaluate the diode behavior and charge transport mechanism [12]. The space-charge-limited current (SCLC) model was applied to analyze carrier transport under high-field conditions.

These optimized fabrication and characterization methods ensure a comprehensive evaluation of (Zn, Sn)O thin films for their potential use as buffer layers in photovoltaic and optoelectronic applications.

RESULTS AND DISCUSSION

X-ray Diffraction (XRD) Analysis of Sn/Zn Annealed at Different Temperatures

Figure 1 shows the X-ray diffraction (XRD) patterns of Sn/Zn bilayers annealed at 400°C, 450°C, 500°C, and 550°C reveal significant changes in crystallinity, phase composition, and oxidation state as a function of annealing temperature.

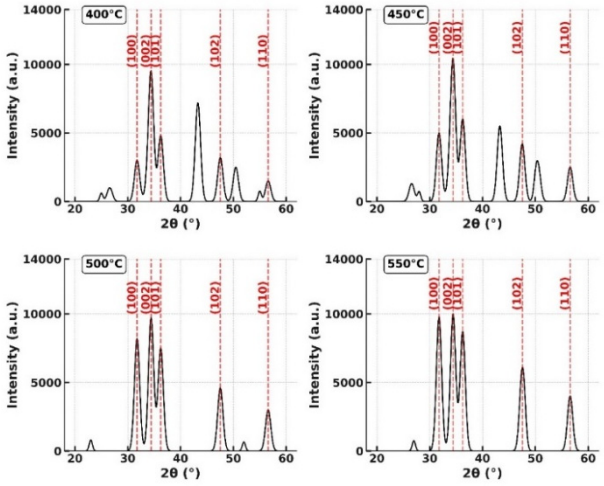

Figure 1. X-ray diffraction (XRD) patterns of (Zn,Sn)O thin films annealed at different temperatures (400°C–550°C)

The diffraction peaks correspond to key crystallographic planes of the hexagonal wurtzite ZnO phase, indexed as (100), (002), (101), (102), and (110). At lower annealing temperatures (400°C and 450°C), the XRD spectra exhibit broad diffraction peaks with lower intensity, indicating a lower degree of crystallinity and incomplete oxidation of the Sn/Zn bilayer. The presence of metallic Zn and Sn peaks suggests that the oxidation process is still in progress. Similar results were reported by R. Ramarajan et al. [13], where Zn, Sn, ZnO, and SnO phases were identified in as-deposited ZTO thin films prepared using a comparable approach. However, the findings of our study demonstrate a distinct advantage due to the simplicity and efficiency of the selected deposition methods, offering a more practical and scalable route for thin-film fabrication. As the annealing temperature increases, the peaks become sharper and more intense, confirming an improvement in crystallinity. At 500°C, most of the metallic Zn and Sn phases disappear, and at 550°C, a well-defined ZnO phase is obtained with strong preferential orientation along the (101) plane.

This trend indicates that increasing the annealing temperature enhances the oxidation process and promotes the formation of a stable ZnO phase. Using the Debye-Scherrer equation:

$$D = \frac{0.9\lambda}{\beta\cos\theta}, \tag{1}$$

where D is the crystallite size, λ is the X-ray wavelength (~1.5406 Å for Cu K α radiation), β is the full width at half maximum (FWHM), and θ is the Bragg angle, an increase in crystallite size with higher annealing temperatures can be inferred [14,15]. This suggests that thermal activation enhances grain growth, reducing microstrain and defect density within the crystal lattice.

The transition from a mixed Sn/Zn phase to a highly crystalline ZnO phase at 500°C and 550°C has direct implications for electrical and optical properties. At lower annealing temperatures, the residual metallic Zn and Sn phases contribute to electrical conductivity, potentially leading to a mixed metallic-semiconducting behavior [16]. However, at 500°C and 550°C, the formation of a well-ordered ZnO phase with improved crystallinity enhances its semiconductor properties, including a widening of the optical band gap (~3.2 eV) and reduced charge carrier scattering.

In summary, the XRD analysis confirms that annealing plays a crucial role in determining the structural and phase composition of ZnO-based thin films. The optimal annealing temperature for obtaining a pure, highly crystalline ZnO phase is 550°C, where a well-ordered wurtzite structure is achieved. This finding is essential for applications in optoelectronics and photovoltaics, where high structural purity and crystallinity are required for efficient charge transport and light absorption.

Figures 2 and 3 illustrate the transmittance and reflectance spectra of Sn/Zn thin films annealed at 400°C, 450°C, 500°C, and 550°C in air for 2 hours. Optical measurements were conducted in the 200–1500 nm wavelength range to analyze how annealing influences the films light absorption, transmission, and reflection characteristics. Similar results were obtained by Acharya et al. [17] for ZTO thin films fabricated using the co-evaporation technique. However, our study highlights the effectiveness of vacuum thermal evaporation followed by annealing, providing a simpler and more controlled approach for achieving high-quality (Zn,Sn)O thin films.

The transmittance spectra (Figure 2) demonstrate a systematic decrease in optical transmission with increasing annealing temperature. At 400°C, the transmittance reaches a peak of ~85% in the near-infrared region (900–1500 nm), but as the annealing temperature rises to 550°C, transmittance declines to ~65% in the same spectral range. This reduction can be attributed to multiple factors: (i) a redshift in the absorption edge from ~370 nm at 400°C to ~410 nm at 550°C, indicative of bandgap narrowing caused by increased carrier concentration and defect incorporation; (ii) enhanced optical absorption due to improved crystallinity and the formation of Sn-rich secondary phases, which introduce localized electronic states acting as additional absorption centers; and (iii) interference fringes in the spectra, suggesting variations in film thickness and refractive index modifications as a function of annealing temperature. At shorter wavelengths (200-500 nm), transmittance is significantly reduced, particularly for films annealed at 550°C, where it falls below 10% at 250 nm, due to strong interband transitions.

The reflectance spectra (Figure 3) indicate a progressive increase in reflectance as the annealing temperature rises, especially in the visible and near-infrared regions (500–1500 nm).

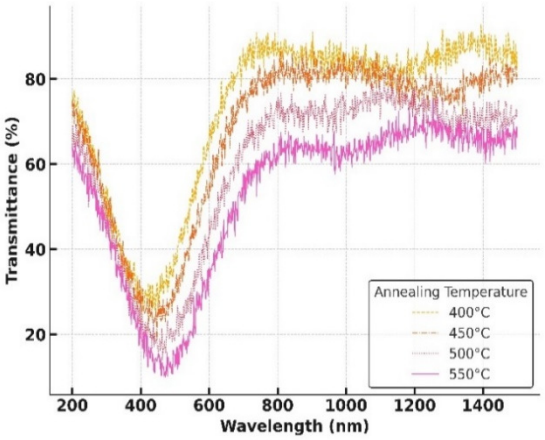

Figure 2. Effect of annealing temperature on the optical transmittance of Zn_2SnO_4 thin films

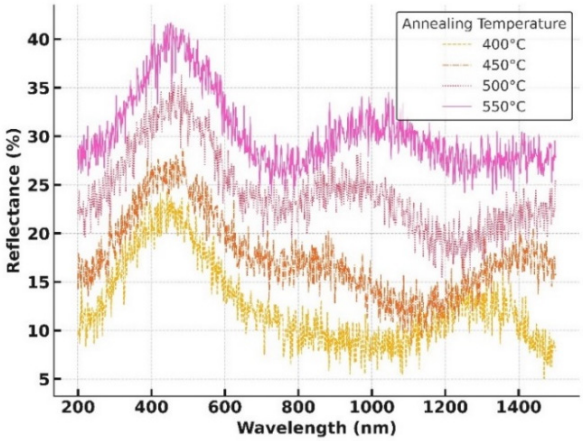

Figure 3. Effect of annealing temperature on the optical reflectance of Zn_2SnO_4 thin films

Reflectance values increase from ~10% at 400°C to ~25% at 550°C, with a more pronounced difference beyond 1000 nm. The observed reflectance enhancement is primarily driven by (i) increased surface roughness, which promotes more diffuse scattering and reflection; (ii) higher free carrier concentration, leading to modifications in the dielectric function and an increase in infrared reflectance due to free carrier absorption; and (iii) structural phase evolution, where a transition from ZnO-dominated films to SnO_2-rich compositions influences the refractive index and light interaction properties. Notably, the reflectance spectra exhibit intersections at ~700 nm and ~1200 nm, indicative of transitions in optical behavior correlated with phase evolution and carrier dynamics.

These findings confirm that annealing temperature plays a crucial role in tailoring the optical properties of Sn/Zn thin films. Increasing the annealing temperature results in decreased transmittance and increased reflectance, primarily due to bandgap narrowing, defect-induced absorption, and carrier concentration variations.

Figure 4 illustrates the dependence of resistivity, carrier concentration, and Hall mobility on doping concentration in (Zn,Sn)O thin films.

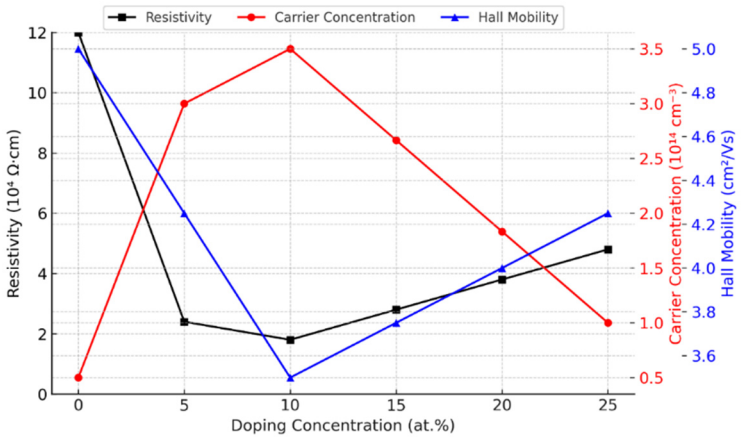

Figure 4. Effect of Sn doping on electrical transport properties of Zn_2SnO_4 thin films

The electrical transport properties of Zn_2SnO_4 thin films, synthesized via vacuum thermal evaporation followed by controlled annealing, were analyzed to understand the dependence of resistivity (Ω·cm), carrier concentration (cm^{-3}), and Hall mobility (cm^2/Vs) on Sn doping concentration (0–25 at.%).

The resistivity **(ρ)** variation follows the classical conductivity relation in semiconductors:

$$\sigma = qn\mu, \tag{2}$$

where $\sigma = 1/\rho$ is the electrical conductivity, q is the elementary charge, n is the carrier concentration, and μ is the Hall mobility [18]. The experimental data show a strong inverse correlation between resistivity and doping concentration up to 10 at.%, indicating an increase in free carrier density. Beyond this, resistivity stabilizes, which suggests the onset of ionized impurity scattering and compensation effects, as described by the Matthiessen's rule, where multiple scattering mechanisms contribute additively to the total resistivity.

The carrier concentration **(n)** increases with Sn doping up to 20 at.%, consistent with the Shockley-Read-Hall (SRH) recombination model, where additional doping introduces donor levels that contribute free electrons to the conduction band. However, at higher doping concentrations, a slight decline in carrier density suggests the formation of compensating defects, such as Sn interstitials (Sn_i^{2+}) or oxygen vacancies (V_O), which act as deep-level traps, reducing the effective carrier density. This behavior is characteristic of heavily doped semiconductors, where self-compensation limits the maximum achievable carrier concentration [19].

The Hall mobility **(μ)** initially decreases with increasing doping concentration due to ionized impurity scattering, following the Brooks-Herring and Conwell-Weisskopf models [20], where mobility is given by:

$$\mu \propto \frac{T^{3/2}}{N_d \ln(1+C/N_d)}, \tag{3}$$

where N_d is the ionized donor concentration, T is the absolute temperature, and C is a constant related to screening effects.

The decrease in mobility up to 15 at.% suggests that increased doping introduces Coulombic scattering centers, degrading transport properties. However, at higher Sn concentrations (≥15 at.%), mobility increases, which indicates a transition to grain boundary-limited conduction, where improved crystallinity reduces carrier scattering at interfaces, enhancing transport pathways. This phenomenon aligns with the Seto model, where grain boundary potential barriers are mitigated at higher doping levels.

Impedance spectroscopy and hot probe measurements confirm that Zn_2SnO_4 remains an **n**-type semiconductor across all doping levels, with a conduction mechanism primarily governed by ionized impurity and grain boundary scattering. The observed trends highlight the role of doping-induced defect states, band edge modifications, and charge compensation effects in determining the electrical transport properties of Zn_2SnO_4 thin films.

Electrical Behavior and Transport Mechanisms in Ni-Zn_2SnO_4-pSi-Ni Heterostructures

Figure 5 presents the temperature-dependent I-V characteristics of Ni- Zn_2SnO_4-Si-Ni heterostructures measured at different annealing temperatures (350°C, 400°C, 450°C, 500°C, and 550°C). The logarithmic scale indicates variations in current conduction behavior as a function of applied voltage, highlighting the influence of annealing temperature on electrical properties. In heterostructures, a direct current (DC) flow occurs when the nickel electrode is connected to the positive terminal, with the current being influenced by monopolar injection of charge carriers. This behavior is observed in the logarithmic coordinate system of the volt-ampere characteristics (VAC), where the current-voltage curve displays distinct **l**inear**,** quadratic, and sharp increases in current, suggesting different conduction regimes. The presence of monopolar injection indicates that charge transport is facilitated by electrons injected from the silicon side, with the flow

being restricted by spatial charge traps within the dielectric material and at the dielectric-semiconductor interface. This implies that in the Ni-Zn_2SnO_4-pSi-Ni heterostructures, the current is likely carried by electrons injected from silicon.

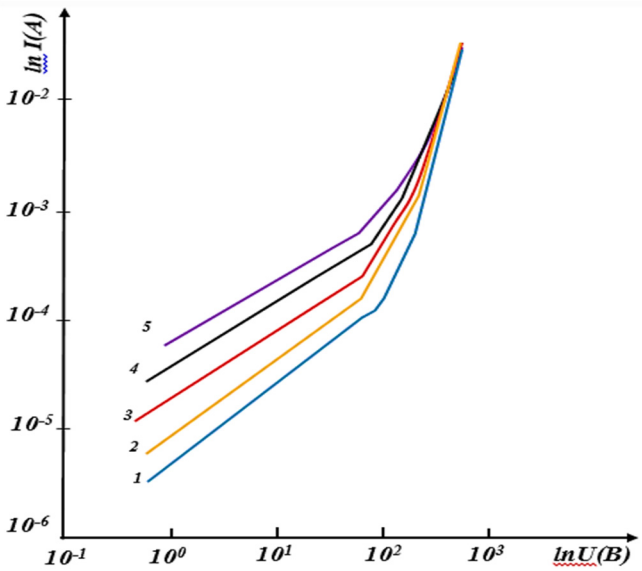

Figure 5. Temperature-dependent I-V characteristics of Ni-Zn_2SnO_4-Si-Ni heterostructures at the following temperatures: 1- 350 °C; 2- 400 °C; 3- 450 °C; 4- 500 °C; 5- 550 °C

The VAC of these structures reveals a three-part behavior: ohmic (I(U)), quadratic ($I(U^2)$), and exponential increase in current ($I(U^m+1)$), where m > 2. The current flow from silicon is mainly attributed to the injection of electrons from the silicon side into the Ni-Zn_2SnO_4 layer. The quadratic region in the VAC is expressed by the following relation for monopolar injection [21]:

$$J = \frac{9\epsilon\mu\theta U^2}{8d^3} \quad , \tag{4}$$

where **ε** is the dielectric constant, μ is the drift mobility, U is the applied voltage, d is the thickness of the layer, and θ is the injection factor.

With values of ε = 8.3, μ ≈ 12.0 $cm^2/V{\cdot}s$, d = 1 × 10^{-4} cm, J = 1.9 × 10^{-2} A/cm^2, and U = 30 V, the injection factor θ can be estimated as:

$$\theta = \frac{8Jd^3}{g\epsilon\mu U^2} = 3.3 \times 10^{-5} \quad . \tag{5}$$

This low injection factor suggests the presence of high trap concentrations within the Zn_2SnO_4 layer and at the Zn_2SnO_4-pSi interface. The trap concentration is calculated using the formula:

$$N_t = \frac{2\epsilon U}{ed^2} \quad , \tag{6}$$

which results in a value of N_t = 3.82 × 10^{16} cm^{-3} . Additionally, the trap depth can be estimated as:

$$E_r = \frac{kT\ln N_0}{g\theta N_r} \quad , \tag{7}$$

where N_r is the trap concentration. Based on this calculation, the trap depth is found to be E_r = 0.45 eV.

When the nickel electrode is connected to the negative terminal, electrons are injected into the Zn_2SnO_4 layer, which exhibits a high resistance. The VAC in this case shows linear characteristics on a $\ln I$ and $\sqrt{U}$ coordinate system, which strengthens with increased temperature. This behavior can be explained by the Schottky barrier mechanism. To determine the potential barrier height between Zn_2SnO_4 and Ni, the temperature dependence of VAC was studied. The potential barrier height is calculated using the formula:

$$\phi_B = -kT\ln\frac{I_0}{SAT^2} \quad . \tag{8}$$

The value of Φ_B is found to be 0.75 ± 0.085 eV. Notably, the VAC shows Schottky characteristics up to 10 V, but the current growth slows with increasing voltage, which might be related to tunneling effects or mixed conduction.

In the Ni-Zn_2SnO_4-Si-Ni heterostructures, when the aluminum electrode is connected to the positive terminal, the current is determined by monoenergetic traps (with E_a = 0.45 eV, N_t = 3.82 × 10^{16} cm^{-3}). When the aluminum electrode

is connected to the negative terminal, the main role is played by the Ni-Zn_2SnO_4 interface, with the VAC explained by the Schottky mechanism. This behavior is linked to the p-n junction formed between the Zn_2SnO_4 and p-Si layers, where charge carrier motion is enhanced in the forward direction and significantly limited in the reverse direction. These characteristics ensure the effective use of the heterostructure as a rectifier in electronic circuits, optoelectronic devices, and photovoltaic systems [22].

CONCLUSIONS

In this study, the structural, optical, and electrical properties of (Zn,Sn)O thin films were systematically investigated for their potential application as buffer layers in photovoltaic devices. The films were synthesized via thermal evaporation followed by a controlled oxidation process in an oxygen-rich environment. Post-deposition annealing at varying temperatures (400°C–550°C) played a crucial role in enhancing crystallinity and phase stability. X-ray diffraction (XRD) analysis confirmed the successful formation of a Zn_2SnO_4 phase, with the optimal crystalline quality observed at 550°C.

Optical characterization revealed a bandgap narrowing effect with increasing annealing temperature, attributed to enhanced carrier concentration and defect states. The transmittance spectra indicated a systematic decrease in transparency, while reflectance measurements demonstrated an increase in optical scattering at higher annealing temperatures, affecting the film's light absorption properties – an essential factor in photovoltaic applications.

Electrical measurements, including Hall effect and I-V characterization, highlighted the impact of annealing on charge transport properties. The carrier mobility and conductivity exhibited significant improvements at optimized annealing conditions, with the space-charge-limited current (SCLC) model supports the conclusion that carrier injection is the dominant conduction mechanism in Ni-(Zn,Sn)O-pSi-Ni heterostructures. Additionally, impedance spectroscopy and hot probe measurements established the n-type conductivity of the Zn_2SnO_4 films across all doping levels, with transport mechanisms primarily governed by ionized impurity and grain boundary scattering.

The findings demonstrate that (Zn,Sn)O thin films exhibit excellent optoelectronic properties, making them viable candidates for integration as buffer layers in photovoltaic devices. The ability to tailor crystallinity, bandgap energy, and charge transport characteristics through annealing and doping provides an avenue for optimizing their performance in next-generation solar cells and optoelectronic applications. Further research should focus on doping-induced modifications to refine defect engineering strategies and enhance charge carrier mobility for improved device efficiency.

ORCID

Fakhriddin T. Yusupov, https://orcid.org/0000-0001-8937-7944
Tokhirbek I. Rakhmonov, https://orcid.org/0000-0002-6080-6159
Dadakhon Sh. Khidirov, https://orcid.org/0000-0003-1391-4250
Shakhnoza Sh. Akhmadjanova, https://orcid.org/0009-0002-1568-3281
Javoxirbek A. Axmadaliyev, https://orcid.org/0009-0001-7753-1462

REFERENCES

[1] M.K. Pham, P.H. Dang, and T.V. Huynh, "Studying the structural, optical, and electrical characteristics of Zn2SnO4 films using a direct current magnetron sputtering method," Ceramics International, **50**(4), 6824-6835 (2023). https://doi.org/10.1016/j.ceramint.2023.12.026

[2] N.M. Martin, T. Törndahl, M. Babucci, F. Larsson, K.A. Simonov, D. Gajdek, L.R. Merte, *et al*., "Atomic Layer Grown Zinc-Tin Oxide as an Alternative Buffer Layer for Cu2ZnSnS4-Based Thin Film Solar Cells: Influence of Absorber Surface Treatment on Buffer Layer Growth," ACS Applied Energy Materials, **5**(11), 13971–13980 (2022). https://doi.org/10.1021/acsaem.2c02579

[3] E. Gnenna, N. Khemiri, and M. Kanzari, "Development and characterization of (Zn,Sn)O thin films for photovoltaic application as buffer layers," SN Appl. Sci. **2**(2), 1–9 (2020). https://doi.org/10.1007/S42452-020-1971-5

[4] Z.X. Mirzajonov, K.A. Sulaymonov, T.I. Rakhmonov, F.T. Yusupov, D.Sh. Khidirov, and J.S. Rakhimjonov, "Advancements in Zinc Oxide (ZnO) thin films for photonic and optoelectronic applications: a focus on doping and annealing processes," E3S Web of Conferences, **549**, 03013 (2024). https://doi.org/10.1051/e3sconf/202454903013

[5] N.A. Sultanov, Z.X. Mirzajonov, F.T. Yusupov, and T.I. Rakhmonov, "Nanocrystalline ZnO Films on Various Substrates: A Study on Their Structural, Optical, and Electrical Characteristics," East European Journal of Physics, (2), 309-314 (2024). https://doi.org/10.26565/2312-4334-2024-2-35

[6] F.T. Yusupov, T.I. Rakhmonov, M.F. Akhmadjonov, M.M. Madrahimov, and S.S. Abdullayev, "Enhancing ZnO/Si Heterojunction Solar Cells: A Combined Experimental and Simulation Approach," East European Journal of Physics, (3), 425-434 (2024). https://doi.org/10.26565/2312-4334-2024-3-51

[7] N.E. Sung, H.K. Lee, K.H. Chae, J.P. Singh, and I.J. Lee, "Correlation of oxygen vacancies to various properties of amorphous zinc tin oxide films," J. Appl. Phys. **122**, 085304 (2017). https://doi.org/10.1063/1.5000138

[8] Shajan, Nirmal and Dhanasingh, Bharathi Mohan, "RF magnetron sputtering of Zn2SnO4 thin films: optimising microstructure, optical and electrical properties for photovoltaics," Journal of Materials Science: Materials in Electronics, **35**, 882 (2024). https://doi.org/10.1007/s10854-024-12648-8

[9] V.V. Ganbavle, M.A. Patil, H.P. Deshmukh, and K.Y. Rajpure, "Development of Zn2SnO4 thin films deposited by spray pyrolysis method and their utility for NO2 gas sensors at moderate operating temperature," J. Anal. Appl. Pyrolysis, **107**, 233-241 (2014). https://doi.org/10.1016/j.jaap.2014.03.006

[10] B. Zaidi, N. Houaidji, A. Khadraoui, S. Gagui, C. Shekhar, Y. Özen, K. Kamli, *et al*., "Structural, Optical and Electrical Properties of ZnxSn1-xS Thin Films Deposited by Chemical Spray Pyrolysis," Journal of Nano Research, **61**, 72–77 (2020). https://doi.org/10.4028/WWW.SCIENTIFIC.NET/JNANOR.61.72

[11] X. Li, Z. Su, S. Venkataraj, S.K. Batabyal, and L.H. Wong, "8.6% Efficiency CZTSSe solar cell with atomic layer deposited Zn–Sn–O buffer layer," Sol. Energy Mater. Sol. Cells, **157**, 101–107 (2016). https://doi.org/10.1016/j.solmat.2016.05.032
[12] M.K. Jayaraj, K.J. Saji, K. Nomura, T. Kamiya, and H. Hosono, "Optical and electrical properties of amorphous zinc tin oxide thin films examined for thin film transistor application," J. Vac. Sci. Technol. B, **26**, 495 (2008). https://doi.org/10.1116/1.2839860
[13] R. Ramarajan, M. Kovendhan, D.T. Phan, K. Thangaraju, R.R. Babu, K.J. Jeon, and D.P. Joseph, "Optimization of Zn2SnO4 thin film by post oxidation of thermally evaporated alternate Sn and Zn metallic multi-layers," Appl. Surf. Sci. **449**, 68-76 (2018). https://doi.org/10.1016/j.apsusc.2018.01.029
[14] M.S. Abd Aziz, M.S. Salleh, G. Krishnan, N. Mufti, M.F. Bin Omar, and S.W. Harun, "Structural, Morphological and Optical Properties of Zinc Oxide Nanorods prepared by ZnO seed layer Annealed at Different Oxidation Temperature," Malaysian Journal of Fundamental and Applied Sciences, **18**(3), 383–392 (2022). https://doi.org/10.11113/mjfas.v18n3.2538
[15] S.W. Chang, K. Ishikawa, and M. Sugiyama, "RF magnetron sputtering deposition of amorphous Zn–Sn–O thin films as a buffer layer for CIS solar cells," Phys Status Solidi C, **12**, 688–691 (2015). https://doi.org/10.1002/pssc.201400255
[16] J.Y. Hwang, and S.Y. Lee, "Effect of Annealing Temperature on Electrical Properties and Stability of Si–Zn–Sn–O Thin Film Transistors Under Temperature Stress," Transactions on Electrical and Electronic Materials, **19**(1), 15–19 (2018). https://doi.org/10.1007/S42341-018-0011-2
[17] R. Acharya, Y.Q. Zhang, and X.A. Cao, "Characterization of zinc–tin–oxide films deposited by thermal co-evaporation," Thin Solid Films, **520**, 6130–6133 (2012). https://doi.org/10.1016/j.tsf.2012.05.087
[18] K. Ellmer, "Hall Effect and Conductivity Measurements in Semiconductor Crystals and Thin Films," in: *Characterization of Materials*, (2012), pp. 1–16. https://doi.org/10.1002/0471266965.COM035.PUB2
[19] A. Treglia, F. Ambrosio, S. Martani, G. Folpini, A.J. Barker, M.D. Albaqami, F. De Angelis, *et al*., "Effect of electronic doping and traps on carrier dynamics in tin halide perovskites," Materials Horizons, **9**(6), 1763–1773 (2022). https://doi.org/10.1039/d2mh00008c
[20] D. Rode, and J. Cetnar, "Electron mobility of heavily doped semiconductors including multiple scattering by ionized impurities," Journal of Applied Physics, **134**, 075701 (2023). https://doi.org/10.1063/5.0165201
[21] N. Sultanov, Z. Mirzajonov, and F. Yusupov, "Technology of production and photoelectric characteristics of AlB 10 heterojunctions based on silicon," E3S Web of Conferences, **458**, 01013 (2023). https://doi.org/10.1051/e3sconf/202345801013
[22] J.H. Lee, B.H. Lee, J. Kang, M.S. Diware, K. Jeon, C. Jeong, S.Y. Lee, and K.H. Kim, "Characteristics and Electronic Band Alignment of a Transparent p-CuI/n-SiZnSnO Heterojunction Diode with a High Rectification Ratio," Nanomaterials, **11**(5), 1237 (2021). https://doi.org/10.3390/NANO11051237

ТОНКІ ПЛІВКИ Zn_2SnO_4 ДЛЯ ФОТОВОЛЬТАЇКИ: СТРУКТУРНА ОПТИМІЗАЦІЯ ТА АНАЛІЗ ПЕРЕНЕСЕННЯ ЗАРЯДУ

Фахріддін Т. Юсупов, Тохірбек І. Рахмонов, Дадахон Ш. Хідіров, Шахноза Ш. Ахмаджонова, Жавохірбек А. Ахмадалієв
Ферганський політехнічний інститут, Фергана, Узбекистан

У цьому дослідженні синтезовано та охарактеризовано тонкі плівки (Zn,Sn)O для потенційного використання як буферних шарів у фотовольтаїчних пристроях. Плівки були осаджені методом термічного випаровування у високовакуумній камері, а потім піддані контрольованому процесу окислення в атмосфері чистого кисню для утворення ZnO-оксидного шару. Післяосадочний відпал проводився при різних температурах (400°C–550°C) для покращення кристалічності та фазового складу. Аналіз рентгенівської дифракції (XRD) підтвердив формування високо-кристалічної фази Zn_2SnO_4, при цьому оптимальна структура була досягнута при 550°C. Оптична характеристика виявила температурно-залежне звуження забороненої зони, що суттєво вплинуло на спектри пропускання та відбивання. Електричні властивості оцінювали за допомогою вимірювань ефекту Холла та струм-напругових (I-V) характеристик, які показали збільшення рухливості носіїв заряду та електропровідності при підвищених температурах відпалу. Механізм перенесення заряду в гетероструктурах Ni-(Zn,Sn)O-pSi-Ni був проаналізований за допомогою моделі струму, обмеженого просторовим зарядом (SCLC), що виявило домінуючі процеси інжекції носіїв заряду. Отримані результати демонструють, що тонкі плівки (Zn,Sn)O мають відмінні оптоелектронні властивості, що робить їх перспективними кандидатами для фотовольтаїчних та оптоелектронних застосувань.

Ключові слова: *(Zn,Sn)O тонкі плівки; фотоелектричні застосування; термічне випаровування; рентгенівська дифракція; оптичні властивості; електротранспорт; ефект Холла; рухливість носіїв заряду; гетероструктури*